Inorganic Chemistry
Communication

Inorg. Chem. **2010**, *49*, 1277–1279 **1277**
DOI: 10.1021/ic901437e

Catalytic Water Oxidation by Single-Site Ruthenium Catalysts

Javier J. Concepcion,* Jonah W. Jurss, Michael R. Norris, Zuofeng Chen, Joseph L. Templeton, and Thomas J. Meyer*

Department of Chemistry, University of North Carolina at Chapel Hill, Chapel Hill, North Carolina 27599

Received July 21, 2009

A series of monomeric ruthenium polypyridyl complexes have been synthesized and characterized, and their performance as water oxidation catalysts has been evaluated. The diversity of ligand environments and how they influence rates and reaction thermodynamics create a platform for catalyst design with controllable reactivity based on ligand variations.

We recently reported that $[Ru(tpy)(bpm)(OH_2)]^{2+}$ and $[Ru(tpy)(bpz)(OH_2)]^{2+}$ (tpy = 2,2′:6′,2″-terpyridine; bpm = 2,2′-bipyrimidine; bpz = 2,2′-bipyrazine) act as single-site catalysts for water oxidation.[1] Mechanistic studies revealed a well-defined, stepwise mechanism featuring proton-coupled electron transfer (PCET),[2,3] a high-oxidation-state $Ru^{V}{=}O^{n+}$ intermediate, which undergoes O---O coupling with H_2O, and a series of peroxidic intermediates. The sequence of reactions is illustrated in Scheme 1.

With mechanistic details established, important questions remain. Is single-site water oxidation catalysis a general phenomenon as suggested by other recent reports?[4,5] What are the factors of molecular and electronic structure that maximize the catalytic rates and turnover numbers?

We report here catalytic water oxidation by a series of single-site polypyridyl ruthenium complexes. The diversity of ligand environments, their influence on the rates and reaction thermodynamics, and the breadth of reactivity are remarkable. They point to a family of catalysts at the molecular scale with reactivity controllable by ligand variations that, by suitable modification, can be incorporated into molecular assemblies, into nanostructured arrays, or at interfaces.

Generic structures are illustrated in Figure 1. They include the previously reported tpy complexes[1] along with acetylacetonate (acac)[6] and carbene derivatives, a series of complexes based on the terdentate ligand 2,6-bis(1-methylbenzimidazol-2-yl)pyridine (Mebimpy), and a series of complexes of the type $Ru(DMAP)(NY)(OH_2)^{2+}$ [DMAP = 2,6-bis[(dimethylamino)methyl]pyridine;[7] NY = 2,2′-bipyridine (bpy), 3-methyl-1-pyridylimidazol-2-ylidene (MeIm-py), and 3-methyl-1-pyridylbenzimidazol-2-ylidene (Mebim-py); see Figure 1].

A special case is $Ru(Mebimpy)(4,4'\text{-}CH_2PO_3H_2bpy)(OH_2)^{2+}$ because phosphonic acid derivatization imparts aqueous stability upon binding to metal oxide surfaces in acidic or neutral environments.

The synthesis and characterization of the series $[Ru(tpy)(LL)(OH_2)]^{n+}$ with LL = bpy, bpm, bpz, and acac were described previously.[1,6,8,9] The synthesis of the series $[Ru(Mebimpy)(LL)(OH_2)]^{n+}$ with LL = bpy, bpm, bpz, and acac was accomplished by procedures similar to those used for the corresponding tpy complexes.[1,8,9] They involved isolation of $[Ru(Mebimpy)(LL)(Cl)]^{n+}$ followed by replacement of the chloro ligand in water assisted by added silver triflate or in neat triflic acid. The *trans*-$[Ru(tpy)(NC)(OH_2)]^{2+}$, *trans*-$[Ru(Mebimpy)(NC)(OH_2)]^{2+}$, and *trans*-$[Ru(DMAP)(NC)(OH_2)]^{2+}$ [NC = MeIm-py, Mebim-py, and 3-methyl-1-pyrazylbenzimidazol-2-ylidene (Mebim-pz)] series were obtained by reaction of the monocationic carbene precursors with $Ru(tpy)Cl_3$,[10] $Ru(Mebimpy)Cl_3$,[9] or $Ru(DMAP)Cl_3$[7] in ethylene glycol at 150 °C in the presence of NEt_3. In these cases, aqua complexes rather than chloro complexes were obtained because of the trans-labilizing effect of the carbene on chloride ligand loss, with the trans isomer the only product; see below. $[Ru(Mebimpy)(4,4'\text{-}(CH_2PO_3H_2\text{-}bpy)(OH_2)]^{2+}$ was prepared by modification of the procedure used to synthesize $[Ru(Mebimpy)(bpy)(OH_2)]^{2+}$, with an extra step required to hydrolyze the phosphonate ester groups. $Ru(DMAP)(bpy)(OH_2)^{2+}$ was prepared following a literature procedure.[7] All complexes were characterized by

*To whom correspondence should be addressed. E-mail: jconcepc@email.unc.edu (J.J.C.), tjmeyer@unc.edu (T.J.M.).

(1) Concepcion, J. J.; Jurss, J. W.; Templeton, J. L.; Meyer, T. J. *J. Am. Chem. Soc.* **2008**, *130*(49), 16462–16463.
(2) Huynh, M. H. V.; Meyer, T. J. *Chem. Rev.* **2007**, *107*(11), 5004–5064.
(3) Meyer, T. J.; Huynh, M. H. V.; Thorp, H. H. *Angew. Chem., Int. Ed.* **2007**, *46*(28), 5284–5304.
(4) Tseng, H.-W.; Zong, R.; Muckerman, J. T.; Thummel, R. *Inorg. Chem.* **2008**, *47*(24), 11763–11773.
(5) Hull, J. F.; Balcells, D.; Blakemore, J. D.; Incarvito, C. D.; Eisenstein, O.; Brudvig, G. W.; Crabtree, R. H. *J. Am. Chem. Soc.* **2009**, *131*(25), 8730–8731.
(6) Dovletoglou, A.; Adeyemi, S. A.; Meyer, T. J. *Inorg. Chem.* **1996**, *35* (14), 4120–4127.
(7) Welch, T. W.; Ciftan, S. A.; White, P. S.; Thorp, H. H. *Inorg. Chem.* **1997**, *36*(21), 4812–4821.
(8) Takeuchi, K. J.; Thompson, M. S.; Pipes, D. W.; Meyer, T. J. *Inorg. Chem.* **1984**, *23*(13), 1845–1851.
(9) Concepcion, J. J.; Tsai, M.-K.; Muckerman, J. T.; Meyer, T. J. *J. Am. Chem. Soc.* **2009**, submitted for publication.
(10) Sullivan, B. P.; Calvert, J. M.; Meyer, T. J. *Inorg. Chem.* **1980**, *19*(5), 1404–1407.

Published on Web 01/08/2010

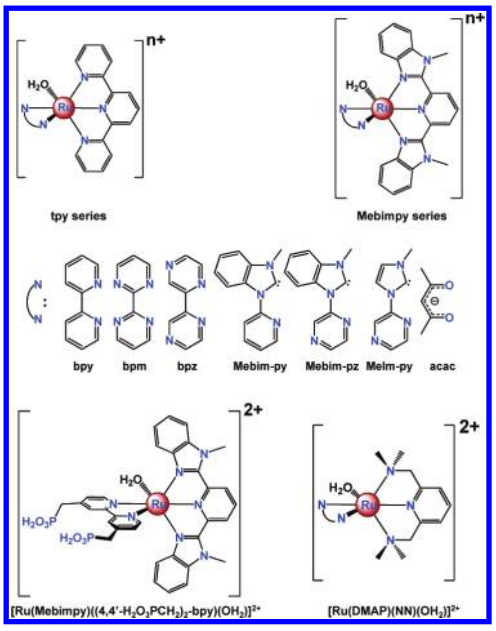

Figure 1. Single-site water oxidation catalysts.

Scheme 1. Single-Site Water Oxidation Mechanism with Ce^{IV} as the Oxidant

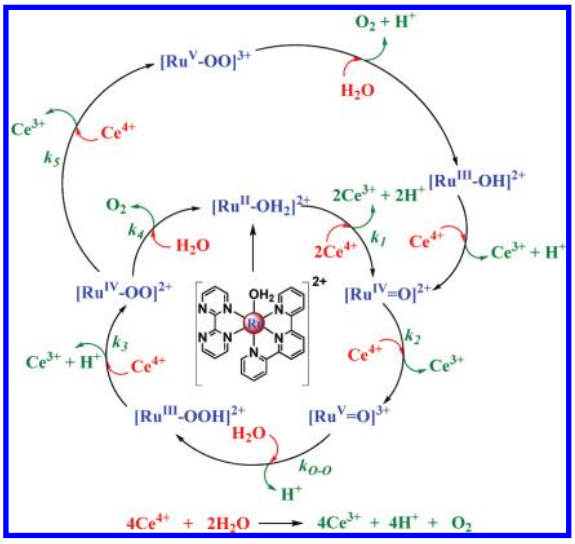

^{1}H NMR, elemental analysis, UV visible absorption spectroscopy, and cyclic voltammetry (see the Supporting Information).

The crystal structure of the *trans*-[Ru(tpy)(Mebim-py)-$(OH_2)]^{2+}$ cation is shown in Figure 2.

As noted above, only the trans isomer was obtained. Notable features in the structure are the relatively short Ru−C distance (1.943 Å) indicative of multiple Ru−C bonding and the longer Ru−O distance (2.183 Å) compared to those of Ru(tpy)(bpy)$(OH_2)^{2+}$ (2.146 Å)[11] and Ru(tpy)-(phendione)$(OH_2)^{2+}$ (2.127 Å; phendione = 1,10-phenanthroline-5,6-dione).[12] This labilizing effect might play an important role in the oxygen evolution step in the water oxidation catalytic cycle.

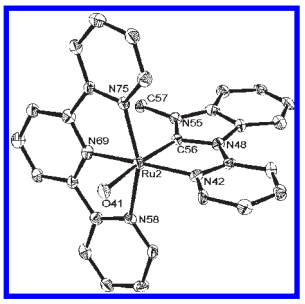

Figure 2. X-ray structure of the *trans*-$[Ru(tpy)(Mebim\text{-}py)(OH_2)]^{2+}$ cation in the salt *trans*-$[Ru(tpy)(Mebim\text{-}py)(OH_2)](ClO_4)_2$.

Representative cyclic voltammograms for the series $[Ru(Mebimpy)(LL)(OH_2)]^{2+}$ (LL = bpy, bpm, bpz) and for $Ru(DMAP)(bpy)(OH_2)^{2+}$ and *trans*-$[Ru(tpy)(Mebim\text{-}py)(OH_2)]^{2+}$ in 0.1 M HNO_3 and for $Ru(tpy)(acac)(OH_2)]^{+}$ are shown in Figures S8 and S9 in the Supporting Information, respectively.

In these cyclic voltammograms, $E^{\circ\prime}$ values for the $[Ru^{III}(Mebimpy)(LL)(OH/OH_2)]^{2+/3+}$/$[Ru^{II}(Mebimpy)(LL)(OH_2)]^{2+}$ and $[Ru^{IV}(Mebimpy)(LL)(O)]^{2+}$/$[Ru^{III}(Mebimpy)(LL)(OH/OH_2)]^{2+/3+}$ couples vary systematically through the series from 0.82 to 1.13 V for the $Ru^{III/II}$ couple and from 1.24 to 1.48 V for the $Ru^{IV/III}$ couple. $E^{\circ\prime}$ values for the $Ru^{III/II}$ and $Ru^{IV/III}$ couples vary from 0.51 to 1.18 V and from 0.74 to 1.54 V, respectively, in the entire series (Tables 1 and 2).

Variations in $E^{\circ\prime}$ are a consequence of the influence of σ-donor ligands in stabilizing higher oxidation states and π-acceptor ligands in stabilizing Ru^{II}.[6,13] Ligand variations also influence the pK_a's of $Ru^{III}OH_2^{3+}$ and $Ru^{II}OH_2^{2+}$, which, in turn, affect the redox potentials due to the pH dependence of the $Ru^{III/II}$ and $Ru^{IV/III}$ couples. An additional $Ru^{V/IV}$, ligand-dependent wave appears as a shoulder from ~1.40 to ~1.72 V at the onset of a catalytic water oxidation wave. Electrocatalytic water oxidation waves well above the background appear for all complexes past 1.3 V.

All complexes were screened as catalysts for net water oxidation by Ce^{IV}, $2H_2O + 4Ce^{4+} \rightarrow O_2 + 4H^+ + 4Ce^{3+}$, by adding 30 equiv of Ce^{IV} to solutions 5.1×10^{-5} M in complex in 0.1 M HNO_3. In these experiments, loss of Ce^{IV} was monitored spectrophotometrically at 360 nm, on the shoulder of λ_{max} = 318 nm for Ce^{IV}, ε = 3070 M^{-1} cm^{-1}. In all cases, complete Ce^{IV} consumption was observed on time scales from < 100 to 20 000 s.

For the series $[Ru(tpy)(LL)(OH_2)]^{n+}$ (Table 1; LL = bidentate ligand) and $[Ru(LLL)(bpy)(OH_2)]^{2+}$ (Table 2; LLL = tpy, Mebimpy, or DMAP) in 0.1 M HNO_3, absorbance−time measurements with Ce^{IV} in pseudo-first-order excess revealed two types of behavior. In one, the rate law was first-order in complex, added initially as $Ru^{II}(OH_2)^{n+}$, and zero-order in Ce^{4+}. The initial oxidation to $Ru^{IV}{=}O^{n+}$ is rapid. On the basis of Scheme 1, this behavior is consistent with either rate-limiting $Ru^{V}{=}O^{(n+1)+}$ oxo attack on H_2O, k_{O-O}, or rate-limiting O_2 loss from $Ru^{IV}(OO)^{n+}$, k_4. The latter is rate-limiting for $[Ru(tpy)(bpm)(OH_2)]^{2+}$- and $[Ru(tpy)(bpz)(OH_2)]^{2+}$-catalyzed water oxidation.[1] In the second type of behavior, the rate law was first-order in $[Ru^{II}(OH_2)^{n+}]$ and first-order in Ce^{4+}. This limit is consistent

(11) Qvortrup, K.; McKenzie, C. J.; Bond, A. D. *Acta Crystallogr., Sect. E: Struct. Rep. Online* **2007**, *E63*(5), m1400–m1401.
(12) Fujihara, T.; Wada, T.; Tanaka, K. *Dalton Trans.* **2004**, *4*, 645–652.
(13) Masllorens, E.; Rodriguez, M.; Romero, I.; Roglans, A.; Parella, T.; Benet-Buchholz, J.; Poyatos, M.; Llobet, A. *J. Am. Chem. Soc.* **2006**, *128*(16), 5306–5307.

Table 1. Water Oxidation Rate Constants and $E_{1/2}$ (V vs NHE) Values for the $Ru^{III/II}$, $Ru^{IV/III}$, and $Ru^{V/IV}$ Couples in the Series $[Ru(tpy)(LL)(OH_2)]^{n+}$ in 0.1 M HNO_3[a]

LL	$Ru^{III/II}$	$Ru^{IV/III}$	$Ru^{V/IV}$	k_{O-O} or k_4 (s^{-1})	k_2 or k_5 (M^{-1} s^{-1})	$t_{1/2}$ (s^{-1})
bpy	1.01	1.19	1.60	1.9×10^{-4}		3650
bpm	1.12	< 1.12	1.65	7.5×10^{-4}		925
bpz	1.22	< 1.22	1.69	1.4×10^{-3}		495
Mebim-py	1.11	1.49	1.70		33	410
Mebim-pz	1.18	1.54	1.72		170	80
acac	0.51	1.14	1.58	5.0×10^{-4}	515	1390, 26

[a] Half-times ($t_{1/2}$) for net Ce^{IV} consumption with $[Ce^{IV}] = 1.5 \times 10^{-3}$ M and $[RuOH_2]^{2+} = 5.1 \times 10^{-5}$ M at 23 ± 2 °C. Only $2e^-$ $Ru^{IV}{=}O^{2+}/Ru^{II}OH_2{}^{2+}$ couples are observed for $[Ru(tpy)(LL)(OH_2)]^{n+}$ (LL = bpm, bpz).

Table 2. As in Table 1 for the Series $[Ru(LLL)(bpy)(OH_2)]^{2+}$

LLL	$Ru^{III/II}$	$Ru^{IV/III}$	$Ru^{V/IV}$	k_4 (s^{-1})	k_2 or k_5 (M^{-1} s^{-1})	$t_{1/2}$ (s^{-1})
tpy	1.01	1.19	1.60	1.9×10^{-4}		3650
Mebimpy	0.82	1.29	1.67		52	260
DMAP	0.54	0.88	1.40		4.1	3315

with either rate-limiting oxidation of $Ru^{IV}{=}O^{n+}$ to $Ru^{V}{=}O^{(n+1)+}$, k_2 in Scheme 1, or rate-limiting oxidation of $Ru^{IV}(OO)^{n+}$, k_5. Evidence for an additional pathway second-order in complex was obtained at high concentrations of complex and will be discussed in a separate manuscript. $[Ru(tpy)(acac)(OH_2)]^+$ is a special case. Both first- and zero-order pathways in Ce^{IV} compete in 0.1 M HNO_3, with the first-order pathway dominating early in the catalytic cycle and the zero-order pathway dominating as Ce^{IV} is depleted.

Tables 1 and 2 present $E_{1/2}$ values for $Ru^{III/II}$, $Ru^{IV/III}$, and $Ru^{V/IV}$ couples as well as rate constants for the rate-limiting steps in water oxidation catalysis by the series $[Ru(tpy)(LL)(OH_2)]^{n+}$ and $[Ru(LLL)(bpy)(OH_2)]^{2+}$. For comparisons among catalysts having different rate-limiting steps, the half times $t_{1/2}$ for consumption of Ce^{IV}, with $Ce^{IV} = 1.5 \times 10^{-3}$ M initially and $[Ru(OH_2)]^{n+} = 5.1 \times 10^{-5}$ M, are also reported.

General trends emerge from the data in Tables 1 and 2. For the $Ru^{V/III}$ couples, of relevance in the O---O bond-forming step (k_{O-O} in Scheme 1), $E_{1/2}(Ru^{V/III}) = 1/2[(E_{1/2}(Ru^{V/IV}) + E_{1/2}(Ru^{IV/III})]$, is dictated largely by the $Ru^{IV/III}$ couple. It is highly tunable ranging from 1.54 to 0.88 V because of its sensitivity to the σ-donor and π-acceptor properties of the ligands. The $Ru^{V/III}$ couple is pH-dependent. $E^{o\prime}$ decreases by −118 mV/pH unit in strongly acidic solutions where the $Ru^{V}{=}O^{n+}/Ru^{III}OH_2{}^{n+}$ couple and by −59 mV/pH unit for the $Ru^{V}{=}O^{n+}/Ru^{III}OH^{(n-1)+}$ couple dominates past the pK_a for $Ru^{III}OH_2{}^{n+}$, which is also ligand-dependent (see Figures S16−S18 in the Supporting Information for representative $E_{1/2}$−pH diagrams).

For representative complexes $[Ru(tpy)(bpm)(OH_2)]^{2+}$, $[Ru(tpy)(Mebim\text{-}py)(OH_2)]^{2+}$, $[Ru(tpy)(Mebim\text{-}pz)(OH_2)]^{2+}$, and $[Ru(Mebimpy)(bpy)(OH_2)]^{2+}$, oxygen evolution was measured by use of an O_2 electrode (Supporting Information). In all cases, the expected amount of oxygen, 7.5 equiv/30 equiv of Ce^{IV}, was observed, showing that water oxidation is quantitative. As illustrated in Figure S9 in Supporting Information for $[Ru(tpy)(acac)(OH_2)]^+$, these complexes are also electrocatalysts with evidence for water oxidation triggered by the oxidation of $Ru^{IV}{=}O^{+}$ to $Ru^{V}{=}O^{2+}$ at slow scan rates.

Our observations are remarkable in pointing to the generality of water oxidation catalysis by single-site ruthenium complex catalysts. Water oxidation appears to occur by a common mechanism utilizing PCET oxidation of Ru^{II}-$(OH_2)^{2+}$ to $Ru^{IV}{=}O^{n+}$, followed by further oxidation and oxo transfer from $Ru^{V}{=}O^{(n+1)+}$ to H_2O to give $Ru^{III}OOH^{n+}$. The O---O bond-forming reaction is reminiscent of well-documented oxygen-atom transfer to sulfides, sulfoxides, phosphines, and olefins by $Ru(bpy)_2(py)(O)^{2+}$ and $Ru(tpy)(bpy)(O)^{2+}$.[14] Water oxidation catalysis appears to be general for polypyridyl aqua complexes with coordinated H_2O, which have oxidatively stable ligands, the ability to reach higher oxidation state Ru=O intermediates, and the driving force to carry out the reaction.

Acknowledgment. Funding by the Chemical Sciences, Geosciences and Biosciences Division of the Office of Basic Energy Sciences, U.S. Department of Energy, Grant DE-FG02-06ER15788, and UNC EFRC: Solar Fuels and Next Generation Photovoltaics, an Energy Frontier Research Center funded by the U.S. Department of Energy, Office of Science, Office of Basic Energy Sciences, under Award DE-SC0001011 is gratefully acknowledged.

Supporting Information Available: Crystallographic data in CIF format, synthetic procedures, oxygen measurements, and electrochemical and kinetic studies. This material is available free of charge via the Internet at http://pubs.acs.org.

(14) Meyer, T. J.; Huynh, M. H. V. *Inorg. Chem.* **2003**, *42*(25), 8140–8160.